



ELSEVIER

Microelectronic Engineering 53 (2000) 667–670

**MICROELECTRONIC  
ENGINEERING**

www.elsevier.nl/locate/mee

## A Liquid-Xenon-Jet Laser-Plasma X-Ray and EUV Source

B. A. M. Hansson\*, L. Rymell, M. Berglund and H. M. Hertz

Biomedical & X-Ray Physics, Royal Institute of Technology,  
SE-100 44 Stockholm, Sweden

We describe a laser-plasma soft-x-ray source based on a cryogenic-xenon liquid-jet target. The source is suitable for extreme ultraviolet (EUV) projection lithography and proximity x-ray lithography (PXL). Absolute calibrated spectra in the 1–2 nm range and uncalibrated spectra in the 9–15 nm range are obtained using a free-standing transmission grating and a CCD-detector.

### 1. INTRODUCTION

The laser-produced plasma is a compact and relatively inexpensive soft x-ray and extreme-ultraviolet (EUV) source. In this paper we describe a xenon liquid-jet laser-plasma source suitable for EUV lithography and proximity x-ray lithography (PXL). This specific source combines the advantages of the microscopic-liquid-jet target method and inert-gas, high-Z target material.

EUV lithography at  $\lambda \sim 11$ –14 nm is currently one of the strongest candidates to succeed deep-ultraviolet lithography for large-scale manufacturing [1–3]. Proximity x-ray lithography at  $\lambda \sim 1$  nm has, for example, found applications in low-volume manufacturing of MMICs [4]. Although synchrotrons are viable sources for both of these short-wavelength lithography systems, the technology would benefit from compact sources with sufficient x-ray or EUV power. The laser-produced plasma is a compact source with the potential to scale to appropriate power levels. Other compact sources under development include z-pinch, capillary discharge and plasma discharge [5].

Laser plasmas are attractive table-top sources due to their small size, high brightness, high spatial stability and, potentially, high-repetition rate. However, with conventional bulk or tape targets, the operating time is limited, especially when high-repetition-rate lasers are used, since

fresh target surfaces cannot be continuously supplied. Furthermore, conventional targets produce debris [6] which may destroy or coat, for example, EUV multilayer optics or x-ray masks that are positioned close to the plasma. Several methods have been designed to eliminate the effect of debris, i.e., preventing the already produced debris from reaching the sensitive components [7]. Instead, the amount of debris produced can be limited by replacing conventional solid targets with, e.g., gas [8], gas-cluster [9], liquid-droplet [10] or liquid-jet [11] targets. A further way to eliminate the coating problem is to use a target consisting of inert atoms [12], i.e. noble gases, so that the debris will not condensate on sensitive components.

Microscopic liquid droplets are attractive low-debris, high-brightness, solid-density targets [10] potentially capable of high repetition-rate operation. Such droplets are generated by stimulated breakup of a continuous jet. The hydrodynamic properties of certain fluids, though, result in unstable drop formation. In that case, the laser can be focused directly onto the jet [11]. It was shown that the debris emission from liquid-jet targets is equally low as from droplet targets. For many gases cooled to their liquid state, droplet formation requires a complicated differential pumping scheme [13] since the jet will freeze long before the droplet formation point due to quick evaporation. Therefore it is preferable to run these cryogenic liquids in the liquid-jet mode. We have previously demonstrated such a cryogenic liquid-

\*e-mail: hansson@physics.kth.se

jet laser-plasma source using nitrogen [14].

In the present paper we report on the first laser-plasma source based on a microscopic liquid-xenon-jet target [15]. A xenon laser plasma has an emission spectrum suitable for both EUV and proximity lithography, and it is a high-Z target promising high conversion efficiency [16]. Furthermore, xenon is an inert gas which should minimize the debris problem. Xenon has earlier been employed as a solid frozen target [12], but it has been shown that a solid xenon target would result in large xenon debris fragments that can damage multilayer optics [17]. Xenon has also been employed as a gas puff target [18] and a gas/cluster target [9]. The latter has been operated at 500 Hz and is being upgraded to 6 kHz [19]. The liquid-jet xenon target, presented here, is a solid-density target still suitable for continuous high-repetition-rate operation. Liquid-jet targets also have the advantage of being high-brightness, low-debris sources and the plasma can be produced far from the nozzle orifice, thereby limiting nozzle erosion.

## 2. EXPERIMENTS AND DISCUSSION

The experimental arrangement for laser-plasma x-ray generation utilizing a liquid-xenon jet as target is shown in Fig. 1. The liquid-xenon jet is formed by forcing xenon gas under 10–50 bars pressure into a small reservoir cooled to 170–200 K by a Gifford-McMahon cold head. A glass capillary nozzle with an orifice of less than 10  $\mu\text{m}$  in diameter is attached to the reservoir, producing a microscopic jet of liquid xenon into a vacuum chamber. Vacuum is maintained with a 1000 l/s turbo drag pump, which typically keeps the chamber pressure at  $10^{-3}$  mbar during operation. In the present experiments no xenon gas recycling was incorporated, although that would be attractive from a cost-of-target perspective.

The plasma-generating laser is a frequency-doubled Nd:YAG laser (Coherent Infinity) delivering 100 Hz of  $\sim 3$  ns long  $\sim 100$  mJ pulses at  $\lambda=532$  nm. The beam is focused onto the xenon jet with a 50 mm lens. Pulse-to-pulse laser-plasma x-ray emission is monitored by an x-ray diode covered by a filter of  $\sim 100$  nm Al

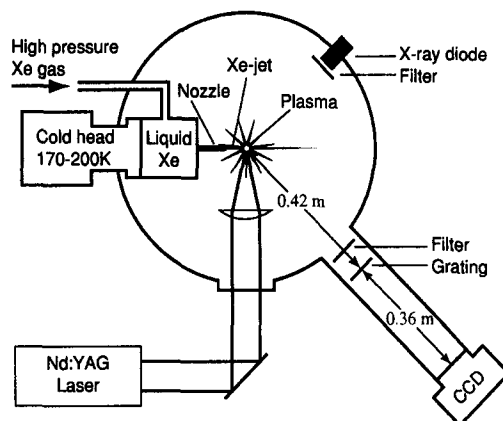


Figure 1. The experimental arrangement

and  $\sim 160$  nm Ag.

Spectra were recorded with a 10000 lines/mm free-standing transmission grating in combination with a cooled, thinned, back-illuminated  $1024 \times 1024$  pixel CCD array (SI003B) [20]. A 0.05 mm slit was mounted in front of the grating resulting in a spectral resolution of  $\Delta\lambda \sim 0.035$  nm. To block the visible radiation, a thin foil of approximately 370 nm zirconium is placed as a filter in front of the grating. The system is calibrated in the  $\lambda=1$ –6 nm wavelength region, thereby allowing absolute photon flux measurements in this wavelength region.

We have operated the xenon-jet in vacuum continuously for several hours. It constitutes a high-density cylindrical target suitable for laser-plasma generation. On average, every second laser pulse hits the jet accurately, making it possible to obtain good spectra although pulse-to-pulse fluctuations are large. The reason for the fluctuations is that the jet undergoes small stochastic changes of direction. Due to the small size of the jet and the laser focus, this instability leads to unstable laser-plasma operation.

Figure 2 shows the xenon spectrum in the  $\lambda=1$ –2 nm region suitable for proximity x-ray lithography. The spectrum has been wavelength cal-

ibrated using published  $\text{Xe}^{26+}$ – $\text{Xe}^{30+}$  emission peaks [21]. Since the transmission grating/CCD system is absolutely calibrated in this wavelength region, the average photon flux can be calculated. The spectrum shows the average flux from a one-second (100 shots) exposure. The conversion efficiency (CE) into the  $\lambda=1\text{--}2$  nm region displayed is  $\sim 2.2\%$  into  $4\pi$  sr, assuming uniform  $4\pi$  sr emission. However, as noted above, only about every second laser pulse hits the jet accurately. Thus, we expect about a factor two improvement of CE and flux once the stability problems have been solved. Furthermore, we have not optimized the laser parameters, making a further improvement of flux and CE likely.

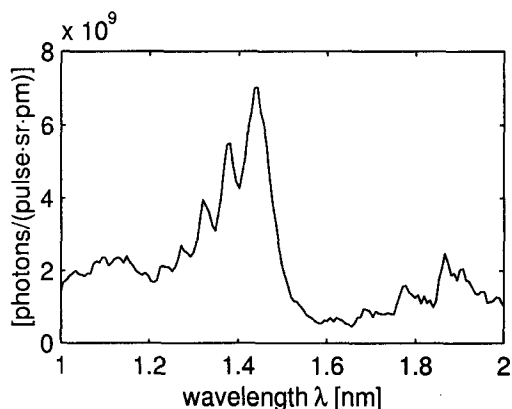


Figure 2. Xe spectrum in the wavelength region suitable for proximity x-ray lithography, showing the average flux of a one-second exposure from a plasma created by 100 Hz of  $\sim 3$  ns long  $\sim 100$  mJ pulses at  $\lambda=532$  nm

Figure 3 shows an emission spectrum in the EUV wavelength region. The spectrum is dominated by the broad band of  $\text{Xe}^{9+}$ – $\text{Xe}^{17+}$  emission centered around  $\lambda=10.8$  nm [22]. The good spectral resolution also permits lines of  $\text{Xe}^{24+}$ – $\text{Xe}^{25+}$  emission to be clearly identified [22]. This high

ionization is probably not ideal from a CE point of view in this wavelength region. Preliminary results actually indicate that lower laser intensities improve the CE. Since the transmission grating is not calibrated in this wavelength region, the spectrum is not corrected for the grating efficiency. The relative intensities in the spectrum are probably not fully correct since the efficiency of the grating is not expected to be constant over the full wavelength range.

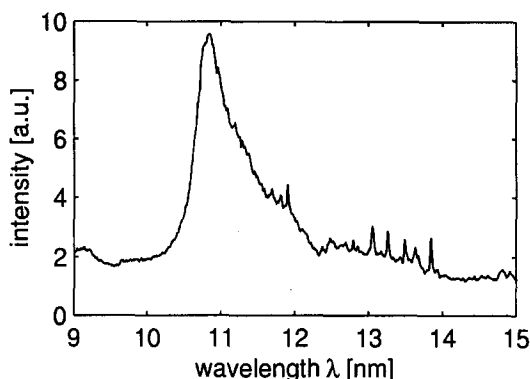


Figure 3. Uncorrected Xe emission spectra in the EUV projection lithography wavelength region.

### 3. CONCLUSIONS

We have demonstrated that cryogenic liquid xenon can be used as a liquid-jet laser plasma target for x-ray and EUV generation. This source holds promise for high-brightness, low debris, high-repetition-rate operation. Future work will focus on absolute flux and conversion-efficiency measurements in the EUV region, and stabilization of the jet.

### REFERENCES

1. J. P. Benschop, W. M. Kaiser and D. C. Ockwell. Y. Vladimirsky (ed.), *Emerging Litho-*

- graphic Technologies III. vol. 3676 of Proceedings of SPIE, (1999) 246.
2. S. Okazaki. Y. Vladimirsky (ed.), *Emerging Lithographic Technologies III*. vol. 3676 of Proceedings of SPIE, (1999) 238.
3. J. E. Goldsmith et al. Y. Vladimirsky (ed.), *Emerging Lithographic Technologies III*. vol. 3676 of Proceedings of SPIE, (1999) 264.
4. R. Selzer and J. Heaton. Using X-ray Lithography to make sub 100 nm MMICs. In this proceeding.
5. V. Y. Banine, J. P. H. Benschop and H. G. C. Werij. Comparison of Extreme Ultraviolet Sources for Lithography Applications. In this proceeding.
6. R. Bobkowski and R. Fedosejevs. *J. Vac. Sci. Technol. B*, 14 (1996), 1973.
7. L. Rymell and H. M. Hertz. *Rev. Sci. Inst.*, 66 (1995), 4916. And references therein.
8. H. Fiedorowicz, A. Bartnik, P. Parys and Z. Patron. P. B. Kenway (ed.), *X-ray optics and microanalysis 1992*. Institute of Physics, Bristol, no. 130 in Institute of Physics conference series, (1993) 515.
9. G. D. Kubiak, L. J. Bernardez, K. D. Krenz, D. J. O'Connell, R. Gutowski and A. M. M. Todd. G. D. Kubiak and D. R. Kania (eds.), *Extreme Ultraviolet Lithography*. vol. 4 of OSA Trends in Optics and Photonics, (1996) 66.
10. L. Rymell and H. M. Hertz. *Opt. Commun.*, 103 (1993), 105.
11. L. Malmqvist, L. Rymell, M. Berglund and H. M. Hertz. *Rev. Sci. Inst.*, 67 (1996), 4150.
12. T. Mochizuki and C. Yamanaka. *Soft X-Ray Optics and Technology* (1986). vol. 733 of Proceedings of SPIE, (1987) 23.
13. M. Tanimoto. *Proceedings of the 7th Symposium on Fusion Technology, Grenoble*. (1972) 267.
14. M. Berglund, L. Rymell, H. M. Hertz and T. Wilhein. *Rev. Sci. Inst.*, 69 (1998), 2361.
15. L. Rymell, M. Berglund, B. A. M. Hansson and H. M. Hertz. Y. Vladimirsky (ed.), *Emerging Lithographic Technologies III*. vol. 3676 of Proceedings of SPIE, (1999) 421.
16. T. Mochizuki et al. *Phys. Rev. A*, 33 (1986), 525.
17. G. D. Kubiak, K. D. Krenz, K. W. Berger, T. G. Trucano, P. W. Fisher and M. J. Gouge. F. Zernike and D. T. Attwood (eds.), *Extreme Ultraviolet Lithography*. vol. 21 of OSA Proceedings, (1995) 248.
18. H. Fiedorowicz et al. *Emerging Lithographic Technologies III*. vol. 2523 of Proceedings of SPIE, (1995) 60.
19. G. D. Kubiak, L. Bernardez, K. Krenz and W. C. Sweatt. Y. Vladimirsky (ed.), *Emerging Lithographic Technologies III*. vol. 3676 of Proceedings of SPIE, (1999) 669.
20. T. Wilhein, S. Rehbein, D. Hambach, M. Berglund, L. Rymell and H. M. Hertz. *Rev. Sci. Inst.*, 70 (1999), 1694.
21. J. F. Wyart, C. Bauche-Arnoult and E. Luc-Koenig. *Phys. Scripta*, 32 (1985), 103.
22. C. Breton et al. *Phys. Scripta*, 37 (1988), 33.